Forensic Chemistry 26 (2021) 100381

Contents lists available at ScienceDirect

Forensic Chemistry

journal homepage: www.sciencedirect.com/journal/forensic-chemistry

Ecstasy tablets: Rapid identification and determination of enantiomeric excess of MDMA

Patrik Fagan [a,*], Dita Spálovská [a], Martin Kuchař [b,c], Tomáš Černohorský [d], Ludmila Komorousová [e], Lucie Kocourková [a,e], Vladimír Setnička [a]

[a] Department of Analytical Chemistry, University of Chemistry and Technology Prague, Technická 5, 166 28 Prague 6, Czech Republic
[b] Forensic Laboratory of Biologically Active Substances, Department of Chemistry of Natural Compounds, University of Chemistry and Technology Prague, Technická 5, 166 28 Prague 6, Czech Republic
[c] National Institute of Mental Health, 250 67 Klecany, Czech Republic
[d] Institute of Environmental and Chemical Engineering, University of Pardubice, Studentská 573, 530 00 Pardubice, Czech Republic
[e] Department of Chemistry, Institute of Criminalistics, Police of the Czech Republic, Bartolomějská 12, 110 00 Prague 1, Czech Republic

ARTICLE INFO

Keywords:
MDMA
Ecstasy
Enantiomeric excess
Electronic circular dichroism
Raman spectroscopy

ABSTRACT

The consumption of psychoactive substances is a worldwide problem and the sheer number of their seizures is alarming. These substances also include the synthetic drug 3,4-methylenedioxy-*N*-methylamphetamine (MDMA), also known as ecstasy, which is very often abused and widespread around the world. The number of ecstasy tablet seizures testifies to their popularity, especially on the dance music scene. One chiral center can be found in the MDMA molecule and therefore it may occur as two enantiomers, which are characterized by different physiological activity. Therefore, knowledge of the enantiomeric excess in the seized tablets is highly desirable. Within the work, dimensional and weight analysis were performed supported by photographic documentation. In addition, Raman and infrared (IR) spectroscopy were used to verify the content of the active substance in the tablets. Subsequently, the electronic circular dichroism (ECD) was used to construct a calibration curve for the determination of the enantiomeric excess of MDMA in the seized tablets. The obtained results show that most of the seized tablets contained MDMA as a racemate.

Introduction

3,4-Methylenedioxy-*N*-methylamphetamine (MDMA, ecstasy) is a synthetic drug belonging to the phenylethylamine group, specifically to the "ecstasy-type" drugs [1,2]. Phenylethylamine is a natural hormone occurring in the human body with effects on the central nervous system. Taking MDMA is characterized by euphoria, increased sensory awareness, mild central stimulation and a weak hallucinogen effect similar to amphetamine. The German company Merck patented MDMA in 1912 [3,4]. After its considerable distribution among users and its negative effect, the United Nations added it to Schedule I of the Single Convention on Narcotic Drugs in 1971 [1,2,5].

MDMA is a chiral molecule (Fig. 1) with one center of chirality and therefore two enantiomers of this substance exist. These enantiomers differ in their binding mechanisms to metabolic enzymes and are characterized by different physiological activity, pharmacokinetics and also neurotoxicity [6]. The (+)-(*S*)-enantiomer is more efficient in the release of monoamines, has a longer duration of action and also higher neurotoxicity than the (−)-(*R*)-enantiomer. On the other hand, the (*R*)–enantiomer has a 4-fold higher affinity for 5-HT_2 receptors than the (*S*)–enantiomer. Since hallucinogens also interact with this type of receptor, the (*R*)-enantiomer is probably responsible for the hallucinogenic effects of MDMA [7–13]. However, due to the very different effects of the individual enantiomers, animal studies have been performed in recent years to investigate the biological activity of the individual enantiomers. The obtained results show that the (*R*)-enantiomer seems to have better properties to become a safe medication for the treatment of post-traumatic stress disorder (PTSD) [14–17], because this enantiomer could be less toxic and less addictive than the (*S*)-enantiomer or racemate [18–22].

MDMA is found most often in the form of salts (hydrochloride or phosphate), sometimes also as a free base. MDMA is very frequently taken among users in the form of tablets with the characteristic logo, less commonly as white powder or crystals. In 2018, approximately

* Corresponding author.
E-mail address: patrik.fagan@vscht.cz (P. Fagan).

https://doi.org/10.1016/j.forc.2021.100381
Received 6 September 2021; Received in revised form 9 November 2021; Accepted 10 November 2021
Available online 15 November 2021

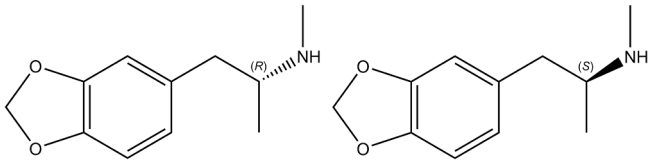

Fig. 1. Structure of (−)-(*R*)-MDMA (left) and (+)-(*S*)-MDMA (right).

13.2 million tablets containing MDMA were seized during 36,000 police raids in the EU, Turkey and Norway. The average content of the active substance in the tablets was in the range of 132–181 mg [2,5,23,24].

In forensic practice, MDMA tablets are very often profiled to determine whether the tablets come from the same manufacturer or even the same batch [25,26]. Tablet profiling can be divided into physical and chemical. Physical profiling includes photo documentation, a description of the tablets' shape, color, dimensions, weight, logos, presence of a score line and especially defects caused during the pressing process [27]. These defects are very important, especially due to the specificity of the press, and arise mainly during the long-term use of the press. Chemical profiling mainly involves the use of fast and non-destructive methods such as IR and Raman spectroscopy for the identification of the active substances and the adulterants [28]. From the ratio of the band intensities of the individual substances, it is possible to identify the same batch and estimate the moisture of the tablets. Subsequently, elemental analysis, gas chromatography (GC) and high-performance liquid chromatography (HPLC) with mass detection (MS) can also be applied to identify impurities (synthesis markers) formed during the synthesis [28–33]. This also helps to reveal the specific synthetic method utilized to produce the MDMA [34,35]. Typically, five synthetic methods are used for the MDMA synthesis, with the Leuckart reaction being the most common type of synthesis employed [36]. Different types of statistical processing can then be applied to evaluate the tablets' profiling. For instance, the method of linear discriminant analysis or advanced multidimensional statistical models may be used for this [37,38].

Whereas the above-mentioned methods do not allow distinction between the individual enantiomers in standard (forensic) practice, the methods of the chiroptical spectroscopy, specifically vibrational circular dichroism (VCD), electronic circular dichroism (ECD), Raman optical activity (ROA) and optical rotation (OR), are appropriate for these purposes. In addition, it is possible to determine the absolute configuration (AC) as well as the enantiomeric excess using these methods [39–54].

In this study, MDMA as an active substance was identified in the seized tablets by Raman and IR spectroscopy supported by GC–MS (GC-FID) and, subsequently, an appropriate procedure based on ECD spectroscopy was developed to determine the enantiomeric excess of MDMA in the seized tablets.

Materials and methods

Chemicals

Standards of both enantiomers of MDMA (enantiomeric excess >99.9%) were synthesized as a hydrochloride in the Forensic Laboratory of Biologically Active Substances (UCT Prague). A total number of 12 seized tablets (Supplementary Data, Fig. S1) was provided by the Police of the Czech Republic, specifically the Institute of Criminalistics. All tablets contained MDMA as the only active substance (Supplementary Data, Table S1) and some achiral excipients, mainly cellulose. For the clarity in this paper, the tablets were labelled as A to L (Table 1). The standard of cellulose was purchased from Sigma-Aldrich, Inc., USA. For ECD spectroscopy, both the enantiomers and seized tablets were dissolved in methanol (MeOH, 99.5%, Sigma-Aldrich Inc., USA). For GC analysis, the *n*-eicosane, cyclohexane, methanol, and sodium carbonate (analytical grade) were purchased from Merck (Germany). The standard of MDMA (≥99.95%, pharmaceutical grade) was purchased from Lipomed (Germany).

Dimensional and weight tablets analysis and photographic documentation

First, the seized tablets were photographed (Supplementary Data, Fig. S1) using a Nikon D 70 (Nikon, Japan) with objective SIGMA 50 mm 1:2.8 DG MACRO D (Sigma, Japan). Subsequently, the seized tablets were weighed on analytical Mettler AE 200 balances (Mettler Toledo, Switzerland) with a precision of 0.5 mg and dimensional analysis was performed using an Extol Premium digital caliper (Extol, Czech Republic) with a precision of 0.02 mm.

Raman and infrared spectroscopy

The standard of MDMA, the seized tablets and powdered (crushed and homogenized) tablets were analyzed by Raman and infrared spectroscopy. Two Raman spectrometers with the excitation wavelengths of 780 and 830 nm were used for this study. These lasers were chosen mainly to identify potential spectral artifacts, evaluate the undesirable fluorescence of MDMA tablet components and to compare two spectrometers – handheld standoff (Pendar X10) and the laboratory spectrometer (DXR SmartRaman). A Pendar X10 handheld standoff Raman system (Pendar Technologies, USA) was used to acquire the Raman spectra in the spectral region of 275–1850 cm^{-1} with a spectral resolution of less than 10 cm^{-1} and equipped with a laser at an excitation wavelength of 830 nm. The system employs shifted excitation Raman difference spectroscopy (SERDS) to overcome the problem of high fluorescence background, which is typical for seized ecstasy tablets. A laser power of 75 mW and beam scanning across the area 2.2 × 2.2 mm were used to avoid photobleaching, lower undesirable fluorescence and negative effects caused by the inhomogeneity of the seized ecstasy tablets and prevent sample degradation. An acquisition time of 200 s was selected after optimization to the best signal to noise ratio.

Table 1
Label of the tablets, tablet stamp and their dimensions and weight.

Tablet label	Tablet stamp	Diameter [mm]	Thickness [mm]	Width [mm]	Height [mm]	Weight [g]
A	681	8.10	3.75	x	x	0.2374
B	656	8.13	4.16	x	x	0.2492
C	A11	8.06	4.98	x	x	0.2918
D	A12	8.08	4.97	x	x	0.3003
E	703	8.14	3.17	x	x	0.2070
F	777	8.30	4.52	x	x	0.2666
G	788	9.00	4.52	x	x	0.3339
H	Donald_Duck	x	5.26	9.92	14.15	0.5375
I	Donkey_Kong	x	5.36	9.11	13.16	0.4586
J	Volkswagen	8.05	4.42	x	x	0.2329
K	Gold	x	3.91	12.14	8.11	0.4346
L	Porsche	x	6.09	9.21	11.09	0.4917

The Raman spectra of the seized tablets at one point (spot less than 1 mm) on the both sides were also measured on a DXR SmartRaman spectrometer (Thermo Scientific, USA) which was equipped with a laser with an excitation wavelength of 780 nm and a diffraction grid comprised of 400 lines per mm. The laser power was set at 75 mW. The final spectra were obtained by averaging 500 scans, each with an exposure time of 3 s (total acquisition time 1500 s). The spectra were measured in a spectral region of 200–3400 cm^{-1} with a resolution of 2.4–4.4 cm^{-1}. The spectra were processed (OMNIC software, Thermo Scientific, USA) with the correction of fluorescence (a 6^{th} order polynomial).

The IR spectra of the standard of MDMA, cellulose and powdered tablets were acquired by a Nicolet iS50 Fourier-transform infrared spectroscopy (FTIR) spectrometer (Thermo Scientific, USA) with a DLaTGS detector, KBr beam splitter and Tungsten-halogen MIR radiation source. The powdered and homogenized seized tablets were analyzed by the attenuated total reflection (ATR) technique with the use of a diamond crystal. The spectra were measured in a spectral region of 4000–450 cm^{-1} with a resolution of 8 cm^{-1} and they are presented as the average of 512 scans. The spectral background was collected before the measurement of each sample.

Electronic circular dichroism and UV absorption spectra

The ECD and UV absorption spectra were measured on a J-815 spectrometer (JASCO, Japan). The spectra were accumulated in a quartz cuvette (Hellma, Germany) with an optical pathlength of 1 mm at ambient temperature in a spectral region of 219–340 nm. First of all, the enantiomerically pure solutions of both enantiomers were prepared with a final concentration of 1.33 $g{\cdot}l^{-1}$ in MeOH and measured as reported previously [49]. Subsequently, these solutions were used for the preparation of the mixtures with different contents stated here for (*R*)-MDMA, specifically 0, 20, 30, 40, 50, 60, 70, 80 and 100% (n/n), for the construction of the calibration curve and the enantiomeric excess determination. The amount of the powdered seized tablets dissolved in MeOH was variable according to the active substance content and was normalized to the same intensity of the UV absorption bands at 286.5 and 236 nm. Besides, cellulose was also analyzed as the major excipient in the spectral region of 219–340 nm where it was confirmed that this substance is achiral (zero CD signal). The following parameters for all the ECD/UV absorption measurements were set: scanning speed 50 $nm{\cdot}min^{-1}$, response time 8 s, bandwidth 1 nm, and sensitivity 100 mdeg. Nineteen accumulations were averaged and these final spectra were corrected for the baseline by subtracting the spectra of the solvent measured under the same experimental conditions.

Gas chromatography

GC-FID analysis

Firstly, an appropriate amount of *n*-eicosane was dissolved in a cyclohexane to obtain a concentration of 0.5 $g{\cdot}l^{-1}$. This solution was used as an internal standard (ISTD). Typically, 20 mg of homogenized samples of MDMA tablets were dissolved in 10 ml of ISTD solution and then 2 ml of water solution of Na_2CO_3 (20% w/w) was added. These solutions of samples were vortexed extensively for 30 min and centrifuged subsequently. A volume of 1–1.5 ml was removed from a top organic part of samples to analytical vials. Such prepared samples were measured by GC with a flame ionization detector (FID).

The GC analyses were performed using a GC-FID Agilent 6890 N with automatic sampler ALS 7683B (both Agilent, USA). The GC separations were carried out on a capillary column DB-5 (25 m × 250 μm × 0.25 μm, Agilent, USA). The carried gas was hydrogen with an average velocity of 83.76 $cm{\cdot}s^{-1}$. The H_2 flow was set to 30.0 $ml{\cdot}min^{-1}$. The samples (1 μl) were injected using syringe of 10 μl by automatic sampler, with a split ratio 12.5:1 and a total flow of 43.5 $ml{\cdot}min^{-1}$ in the injector. The column temperature was going up from 140 °C (maintained for 3 min) to 300 °C at a rate of 45 $°C{\cdot}min^{-1}$.

The quantification was done using method of internal calibration with ISTD (*n*-eicosane). From each pill of MDMA, two samples were prepared by the procedure mentioned above and then the GC separation was performed twice from each prepared sample. Final results are an arithmetic average from four results for each sample. The data evaluation was carried out using OpenLab (Agilent, USA).

GC–MS analysis

The samples for GC–MS analysis were prepared by dissolving 1 mg of homogenized pills in 0.5–1 ml methanol. Then, ones were vortexed (for 10 min) and centrifuged (for 6 min). From such prepared analytes, the volume of 30 μl was removed to analytical vial with 0.5–1 ml pure methanol.

The GC–MS system consisted of an Agilent 6890 N (GC) – mass selective detector 5975B iXL with an automatic sampler ALS 7683B (Agilent, USA). Data handling and system operations were controlled by the MassHunter software (Agilent, USA). The separations were carried out on column HP-5MS 5% phenyl-methyl silox (Agilent 190091S-433, USA) about dimensions' 30 m × 250 μm × 0.25 μm. The injector and transfer line temperatures were 250 and 285 °C, respectively. The oven temperature was programmed from 60 °C (hold time 1 min) to 180 °C at 30 $°C{\cdot}min^{-1}$ and from 180 °C to 280 °C (hold time 5 min) at 10 $°C{\cdot}min^{-1}$. Helium was used as the carrier gas with a total flow of 28.688 $ml{\cdot}min^{-1}$. The scan range was *m/z* 25–550 and the scanning rate set on normal scanning.

Results and discussion

Dimensional, weight and photographic documentation

In total, 8 of the 12 seized tablets were round in shape (Supplementary Data, Fig. S1). All of the tablets were stamped with different logos and symbols. The score line on the backside was perceptible on all tablets, except for the tablets E and J. Some of the logos took the form of a well-known brand or various characters, for example from movies or series. The tablets were significantly different in color.

The diameter of the round tablets was in most cases ~ 8 mm, with the exception of the tablet G with the diameter of 9 mm (Table 1). These similarities were probably caused by the availability of hand presses for compressing the tablets. The tablets H, I and K did not have a circular shape and their width ranged from 9.11 to 12.14 mm. Their height then ranged from 8.11 to 14.15 mm. The thickness of all tablets was relatively variable and the values ranged from 3.75 to 5.36 mm.

The weight of the tablets ranged from 0.2070 to 0.5375 g. The tablets with a circular shape were characterized by a lower weight when compared to the tablets with a non-circular shape.

Raman spectroscopy

First, the Raman spectra of the untreated tablets were measured on each side of the tablet to determine the homogeneity of the tablets. Seized ecstasy tablets are often inhomogeneous and beam scanning can significantly improve the homogeneity of the spectral information in comparison with traditional Raman spectrometers, which use small laser spots. The comparison of the two spectrometers showed (Supplementary Data, Fig. S5) that the spectra of the tablets A and E obtained from two points on the tablet with the traditional Thermo DXR spectrometer (spot size less than 1 mm) were different. On the other hand, the Pendar X10 spectrometer (scanned area 2.2 × 2.2 mm) was able to produce almost the same spectra from different points and it is obvious that it can be used for testing the differences between the sides of tablets (macro inhomogeneity). The obtained results by the Pendar X10 (Supplementary Data, Figs. S2–S4) showed that all provided tablets had the same composition on both sides. The band intensities and spectral pattern on both sides of the tablets B, F and J were almost the same. In

the case of the tablets A, C, E, I, K, and L, the spectral intensities of all bands were higher on one side than on the other, which might be caused by the different focusing of the laser during the measurement of the tablets. However, for the tablets D, G, and H, the intensities of the individual bands differed from both sides, which testified to the different representation of the individual substances and the inhomogeneity of the tablets. Generally, another frequently observed problem is a generation of extremely high fluorescence in the case of the ecstasy tablets, but difference Raman spectroscopy (SERDS) can suppress this undesirable effect with high efficiency. Fig. S6 in Supplementary Data shows the comparison of the spectra of tablets G and L obtained with the Thermo DXR spectrometer (excitation wavelength 785 nm) and the Pendar X10, which was able to produce high fidelity spectra in a 200 s measurement. We also tested the Progeny ResQ FLX (Rigaku, Japan) spectrometer with a 1064 nm excitation laser. Unfortunately, we observed quick thermal decomposition (sample burning at 300 mW; lower laser power provided insufficient spectra quality in terms of signal to noise ratio) for several samples although short integration time and compromise laser power were used, so this technology was not suitable for our experiments. For these reasons, the Pendar X10 spectrometer was used for the subsequent experiments.

Afterward, the Raman spectra of the powdered and homogenized tablets were measured (Figs. 2 and 3) and these spectra were compared with the spectrum of the MDMA standard to confirm the content of the active substance. The identification was performed using the characteristic bands (red vertical line in Figs. 2 and 3), namely band 1 (340 cm^{-1}) reflecting the vibration of the C–N–C group and bands 2 and 4 (535 and 775 cm^{-1}) reflecting the vibration of the C–O–C group. Then, we considered bands 5, 6 and 7 (813, 1371 and 1444 cm^{-1}) to be asymmetric and rocking vibrations of the aliphatic parts of the molecule. We also observed the vibrations of the aromatic ring along with the vibration of the NH group as bands 3, 8 and 9 (720, 1610 and 1633 cm^{-1}). The active substance was identified in all studied tablets. Cellulose the most frequently used adulterant (green line in Figs. 2 and 3) by band 1́, 2́ and 3́. In general, lactose is other commonly used adulterant. These results were consistent with GC analysis (Supplementary Data, Table S1). Two additional bands (1542 and 688 cm^{-1}) were present in the spectrum of tablet H, which have not yet been assigned to a specific impurity. However, we know from the ECD analysis that all the tablet impurities are achiral. Thus, it did not affect the main analysis of enantiomeric excess.

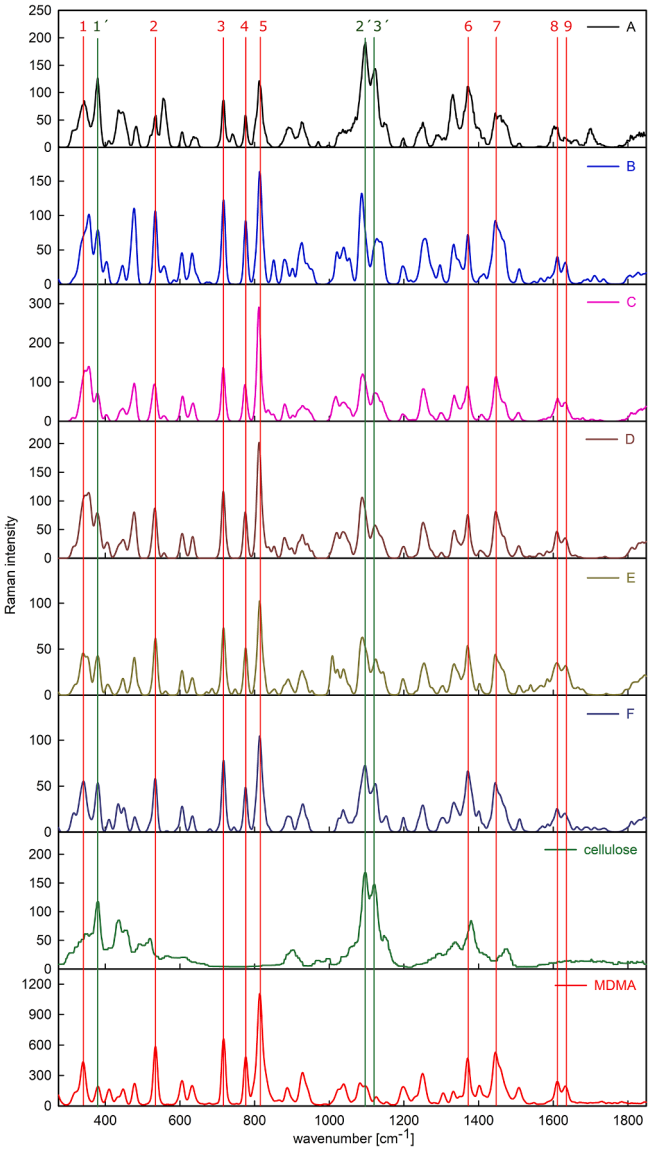

Fig. 2. Raman spectra of the homogenized tablets A, B, C, D, E, F, standards of cellulose and MDMA obtained by the Pendar X10 spectrometer in the spectral region of 275–1849 cm^{-1}. Vertical lines indicate the bands used for identification of MDMA (red lines) and cellulose (green lines). (For interpretation of the references to color in this figure legend, the reader is referred to the web version of this article.)

ATR-FTIR spectroscopy

ATR-FTIR spectroscopy was used to verify the presence of MDMA in the seized tablets. The measured spectra of the powdered and homogenized tablets were compared with the standard of MDMA and the fingerprint region was used for the identification of the active substance (Figs. 4 and 5). For the IR spectra in the extended spectral region (4000–450 cm^{-1}), see Figs. S7 and S8 in Supplementary Data. The characteristic bands 1, 2, 3 and 9 (1483, 1436, 1387 and 799 cm^{-1}) reflecting the vibrations of the aliphatic parts of the molecule and also the vibrations of the aromatic ring in the case of band 2, were used for the identification of MDMA in the tablets (red vertical lines in Figs. 4 and 5). We further observed aromatic methylenedioxy group vibrations, namely bands 4, 5, 7 and 9 (1249, 1190, 1034 and 923 cm^{-1}) and band 6 (1101 cm^{-1}) reflected the vibrations of the C=O group. The active substance could be identified also in the extended spectral range (the bands at 2736 and 2476 cm^{-1}). Finally, the active substance was identified in all studied tablets. These results fully supported those obtained by Raman spectroscopy. The tablet filler used by the producers was identified as cellulose in all of the studied samples. Bands 1́ and 2́ (663 and 537 cm^{-1}) were used for the confirmation of the presence of cellulose in the tablets, due to the fact that there are no MDMA bands in this region (green vertical lines in Figs. 4 and 5). The highest cellulose content was found in tablets B, C and E.

ECD spectroscopy

First, the standards of MDMA in MeOH solution with a different enantiomeric excess were measured. For the construction of the calibration curve, two bands in the range of 220–258 nm were used (Fig. 6). These bands were integrated to obtain their areas, which were used to construct the calibration curve. The integration was performed by the Spectra Manager program (JASCO, Japan). This calibration curve contained 9 points (the content of (*R*)-enantiomer was 0, 20, 30, 40, 50, 60, 70, 80 and 100% (n/n)).

The correlation coefficients were close to unity ($R^2 > 0.9985$) for both selected bands. The enantiomeric excess was calculated as

$$f_{EE} = \frac{c_R - c_S}{c_R + c_S} \cdot 100\%$$

where c_R a c_S means molar concentration of (*R*)- and (*S*)-enantiomer, respectively, and the value +100% means pure (*R*)-enantiomer and

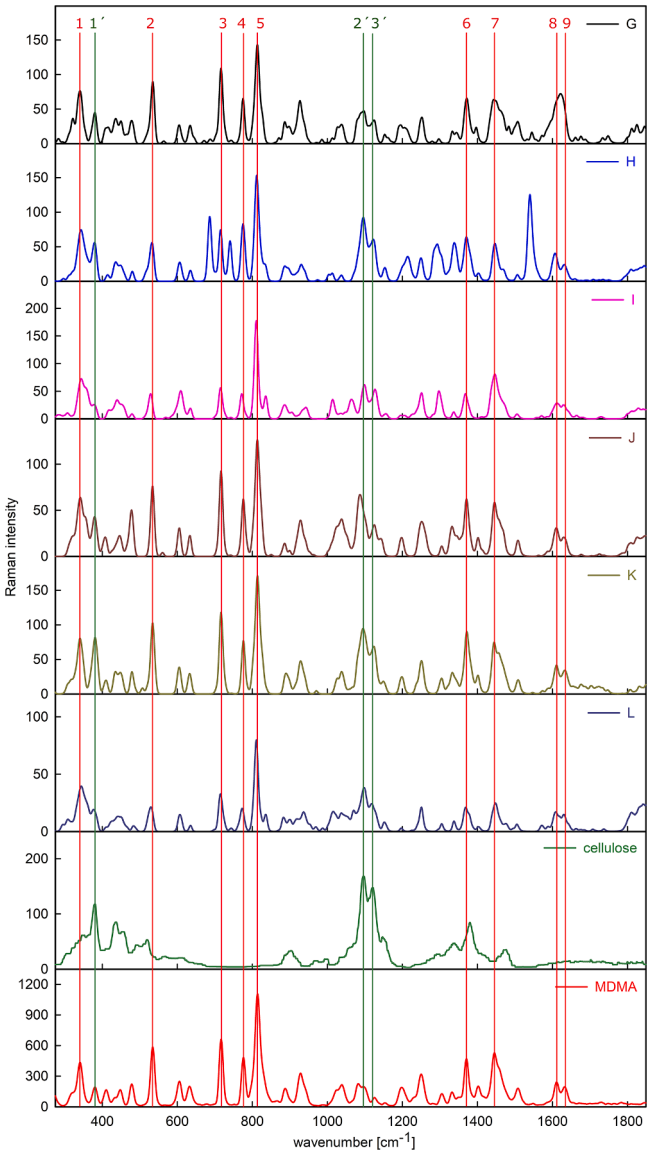

Fig. 3. Raman spectra of the homogenized tablets G, H, I, J, K, L, standards of cellulose and MDMA obtained by the Pendar X10 spectrometer in the spectral region of 275–1849 cm^{-1}. Vertical lines indicate the bands used for identification of MDMA (red lines) and cellulose (green lines). (For interpretation of the references to color in this figure legend, the reader is referred to the web version of this article.)

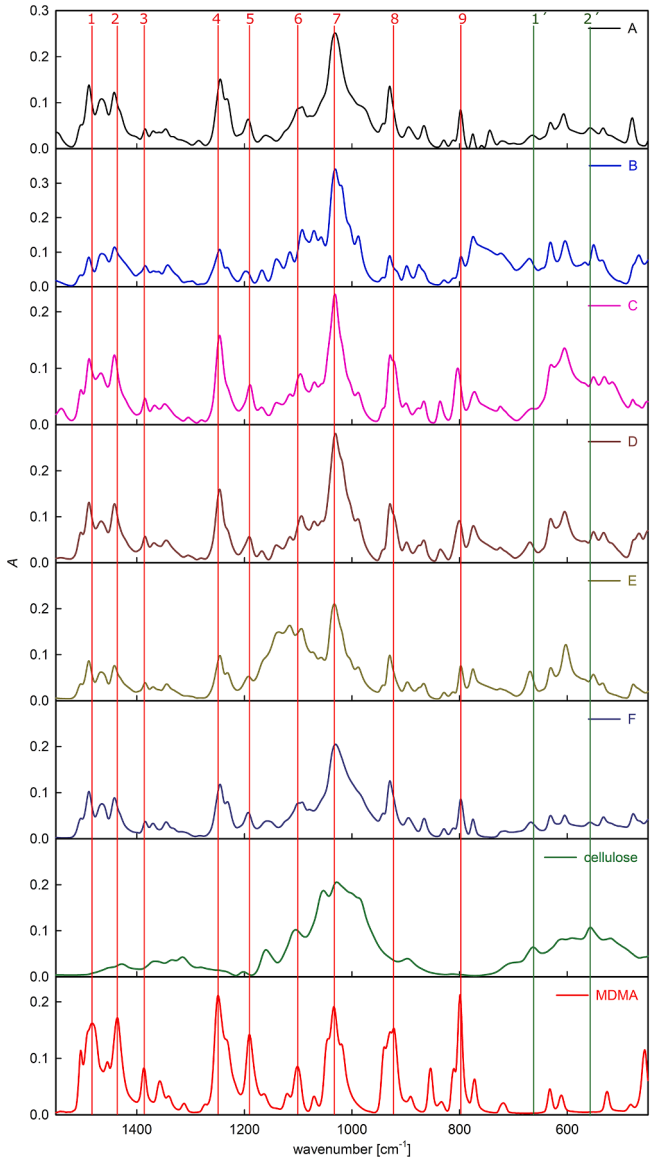

Fig. 4. IR spectra of tablets A, B, C, D, E, F and standards of cellulose and MDMA obtained by the Nicolet iS50 spectrometer in the spectral region of 1550–450 cm^{-1}. Vertical lines indicate the bands used for identification of MDMA (red lines) and cellulose (green lines). (For interpretation of the references to color in this figure legend, the reader is referred to the web version of this article.)

−100% means pure (*S*)–enantiomer. Statistical analysis of enantiomeric excess was used to confirm the validity of these experiments. Two independent values of the enantiomeric excess and their uncertainties for both bands (in the range of 220–258 nm) were determined using regression coefficients with their standard deviations obtained by calibration procedure. Subsequently, the weighted average f^*_{EE} and standard deviations s^* were calculated. The uncertainty of the volumetrically and weighty determined values of f_{EE} were also taken into account for the total evaluation of the deviation of f^*_{EE}. Fig. 7 described the relationship between the ECD measured enantiomeric excess f^*_{EE} and volumetrically determined enantiomeric excess f_{EE} of the prepared calibration solutions, as well as their standard deviations. The standard deviation of f_{EE} was in the range of 1.1–2.2 and for f^*_{EE} in the range of 2.5–3.9.

The results obtained indicated the existence of a linear correlation between the enantiomeric excess and the ECD band area for all the chosen bands. Subsequently, the ECD spectra of the seized tablets were measured and the contents of the individual enantiomers were calculated using the calibration curve (Fig. 8).

Except for tablet G, MDMA was in the form of a racemate in all the analyzed tablets, which was expected (Table 2). The content of the (*R*)-enantiomer was at the level of 50%, including the standard deviations, which were in the range of 3.4–4.8% for all analyzed tablets. However, tablet G contained a significant excess of the (*R*)-enantiomer, namely 63.6% with a standard deviation ± 4.8%.

Conclusion

In this work, the dimensional and weight analysis supported by photographic documentation of the seized MDMA tablets were performed. Subsequently, the active substance was identified by IR and Raman spectroscopy. Moreover, a methodology was developed and a calibration curve with varying content of (*R*)-MDMA constructed to determine the enantiomeric excess of MDMA in those tablets by ECD

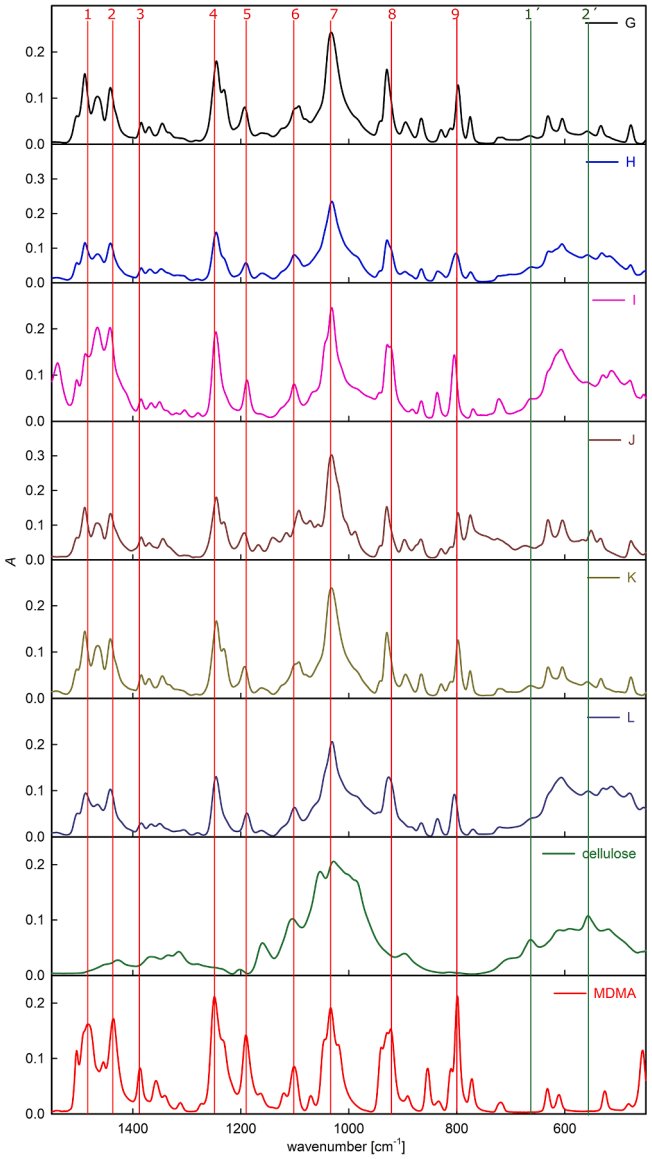

Fig. 5. IR spectra of tablets G, H, I, J, K, L and standards of cellulose and MDMA obtained by the Nicolet iS50 spectrometer in the spectral region of 1550–450 cm^{-1}. Vertical lines indicate the bands used for identification of MDMA (red lines) and cellulose (green lines). (For interpretation of the references to color in this figure legend, the reader is referred to the web version of this article.)

spectroscopy.

The obtained results showed that the circular tablets had a lower weight than the non-circular ones. Using Raman spectroscopy, the front and back sides of the tablets were found to have comparable compositions and the active substance (MDMA) was subsequently identified in all seized studied tablets and confirmed by IR spectroscopy. Last but not least, the ECD spectra of the seized tablets were measured, and it was found that 11 of the 12 tablets contained a racemic mixture of MDMA. However, the content of (*R*)-enantiomer of MDMA was 63.6 % in case of tablet G. The standard deviations were in the range of 3.4–4.8% for all analyzed tablets. Knowledge of the enantiomeric excess of the tablets with non-racemic active ingredient could play an important role in tablet profiling, as the same batch and tablet producer could be revealed from this analysis.

To the best of our knowledge, this is the first study focused on the simple determination of the enantiomeric excess of MDMA in seized tablets.

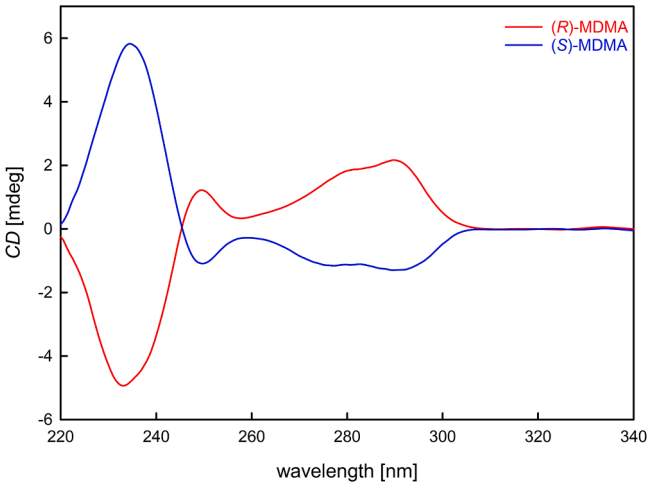

Fig. 6. The ECD spectra of both enantiomers of MDMA in MeOH.

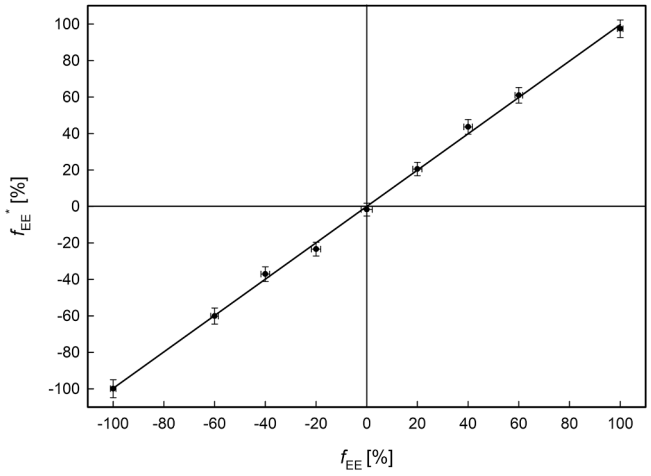

Fig. 7. The calculated f^*_{EE} values (based on the ECD spectra) and volumetrically determined f_{EE} values (calculated for calibration solutions) of enantiomeric excess and their standard deviations.

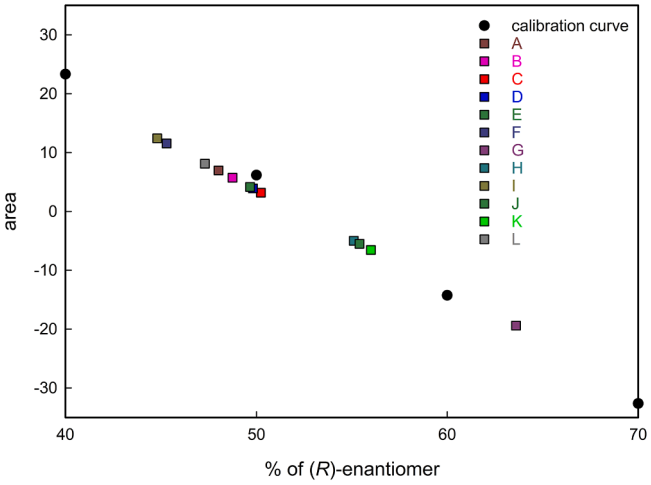

Fig. 8. The calibration points of MDMA made as a correlation of the ECD areas with the content of (*R*)-MDMA (black dots) and content of (*R*)-MDMA in the seized ecstasy tablets (color rectangles).

Table 2
Enantiomeric content of (*R*)-MDMA in tablets and their standard deviations.

Tablet	Content of (*R*)-enantiomer [%]	Standard deviation [%]
A	48.0	±3.6
B	48.7	±3.7
C	50.2	±3.8
D	49.8	±3.7
E	49.7	±3.7
F	45.3	±3.4
G	63.6	±4.8
H	55.1	±4.1
I	44.8	±3.4
J	55.4	±4.2
K	56.0	±4.2
L	47.3	±3.6

Declaration of Competing Interest

The authors declare that they have no known competing financial interests or personal relationships that could have appeared to influence the work reported in this paper.

Acknowledgment

The authors would like to thank Radek Jurok from Forensic Laboratory of Biologically Active Substances (UCT Prague) for the synthesis and enantiomeric separation of MDMA.

Funding

This work was supported by the Ministry of the Interior of the Czech Republic [VJ01010043]. Partial support (infrastructure and instrumentation) was provided from the grant of Specific University Research – grant No A2_FCHI_2021_024.

Ethical approval

This article does not contain any studies with human participants or animals performed by any of the authors.

Appendix A. Supplementary data

Supplementary data to this article can be found online at https://doi.org/10.1016/j.forc.2021.100381.

References

[1] European Monitoring Centre for Drugs and Drug Addiction. *European Drug Report 2018: Trends and Developments*. Luxembourg: Publications Office of the European Union; 2018.
[2] European Monitoring Centre for Drugs and Drug Addiction., *Recent changes in Europeaṅs MDMA/ecstasy market*, Publications Office of the European Union, Luxembourg, 2016.
[3] Verfahren zur Darstellung von Alkyloxyaryl-, Dialkyloxyaryl- und Alkylenedioxyaryl-aminopropanen bzw. Deren am Stickstoff monoalkylierten Derivaten, 1914. German Patent #274350, filed December 24, 1912, issues May 16, 1914, and assigned to E. Merck in Darmstadt.
[4] R.W. Freudenmann, F. Öxler, S. Bernschneider-Reif, The origin of MDMA (ecstasy) revisited: the true story reconstructed from the original documents, Addiction 101 (9) (2006) 1241–1245, https://doi.org/10.1111/j.1360-0443.2006.01511.x.
[5] European Monitoring Centre for Drugs and Drug Addiction. MDMA ('Ecstasy') drug profile https://www.emcdda.europa.eu/publications/drug-profiles/mdma_en#bibliography. Accessed April 20, 2021.
[6] R.G. Pitts, D.W. Curry, K.N. Hampshire, M.B. Young, L.L. Howell, (±)-MDMA and its enantiomers: potential therapeutic advantages of R(−)-MDMA, Psychopharmacology 235 (2) (2018) 377–392, https://doi.org/10.1007/s00213-017-4812-5.
[7] P. Huot, T.H. Johnston, K.D. Lewis, J.B. Koprich, M.G. Reyes, S.H. Fox, M. J. Piggott, J.M. Brotchie, Characterization of 3,4-methylenedioxymethamphetamine (MDMA) enantiomers in vitro and in the MPTP-lesioned primate: R-MDMA reduces severity of dyskinesia, whereas S-MDMA extends duration of ON-time, J. Neurosci. 31 (19) (2011) 7190–7198, https://doi.org/10.1523/JNEUROSCI.1171-11.2011.
[8] M.P. Johnson, A.J. Hoffman, D.E. Nichols, Effects of the enantiomers of MDA, MDMA and related analogues on [3H]serotonin and [3H]dopamine release from superfused rat brain slices, Eur. J. Pharmacol. 132 (2–3) (1986) 269–276, https://doi.org/10.1016/0014-2999(86)90615-1.
[9] R.A. Lyon, R.A. Glennom, M. Titeler, 3,4-Methylenedioxymethamphetamine (MDMA): stereoselective interactions at brain 5-HT1 and 5-HT2 receptors, Psychopharmacology 88 (4) (1986) 525–526, https://doi.org/10.1007/bf00178519.
[10] R.B. Rothman, M.H. Baumann, Monoamine transporters and psychostimulant drugs, Eur. J. Pharmacol. 479 (1–3) (2003) 23–40, https://doi.org/10.1016/j.ejphar.2003.08.054.
[11] R. Moratalla, A. Khairnar, N. Simola, N. Granado, J.R. García-Montes, P. F. Porceddu, Y. Tizabi, G. Costa, M. Morelli, Amphetamine-related drugs neurotoxicity in humansand in experimental animals: main mechanisms, Prog. Neurobiol. 155 (2017) 149–170, https://doi.org/10.1016/j.pneurobio.2015.09.011.
[12] P.C. Dolder, F. Müller, Y. Schmid, S.J. Borgwardt, M.E. Liechti, Direct comparison of the acute subjective, emotional, autonomic, and endocrine effects of MDMA, methylphenidate, and modafinil in healthy subjects, Psychopharmacology 235 (2) (2018) 467–479, https://doi.org/10.1007/s00213-017-4650-5.
[13] D.S. Harris, M. Baggott, J.H. Mendelson, J.E. Mendelson, R.T. Jones, Subjective and hormonal effects of 3,4-methylenedioxymethamphetamine (MDMA) in humans, Psychopharmacology 162 (4) (2002) 396–405, https://doi.org/10.1007/s00213-002-1131-1.
[14] M.T. Wagner, M.C. Mithoefer, A.T. Mithoefer, R.K. MacAulay, L. Jerome, B. Yazar-Klosinski, R. Doblin, Therapeutic effect of increased openness: investigating mechanism of action in MDMA-assisted psychotherapy, J. Psychopharmacol. 31 (8) (2017) 967–974, https://doi.org/10.1177/0269881117711712.
[15] M.E. Liechti, C. Baumann, A. Gamma, F.X. Vollenweider, Acute psychological effects of 3,4-methylenedioxymethamphetamine (MDMA, "Ecstasy") are attenuated by the serotonin uptake inhibitor citalopram, Neuropsychopharmacology 22 (5) (2000) 513–521, https://doi.org/10.1016/S0893-133X(99)00148-7.
[16] M.E. Liechti, F.X. Vollenweider, Acute psychological and psychological effects of MDMA ("Ecstasy") after haloperidol pretreatment in healty humans, Eur. Neuropsychopharmacol. 10 (4) (2000) 289–295, https://doi.org/10.1016/s0924-977x(00)00086-9.
[17] M.C. Mithoefer, M.T. Wagner, A.T. Mithoefer, L. Jerome, R. Doblin, The safety and efficacy of ±3,4-methylenedioxymethamphetamine-assisted psychotherapy in subjects with chronic, treatment-resistant posttraumatic stress disorder: the first randomized controlled pilot study, J. Psychopharmacol. 25 (4) (2010) 439–452, https://doi.org/10.1177/0269881110378371.
[18] S. Schenk, D. Newcombe, Methylenedioxymethamphetamine (MDMA) in psychiatry, J. Clin. Psychopharmacol. 38 (6) (2018) 632–638, https://doi.org/10.1097/JCP.0000000000000962.
[19] K.S. Murnane, W.E. Fantegrossi, J.R. Godfrey, M.L. Banks, L.L. Howell, Endocrine and neurochemical effects of 3,4-methylenedioxymethamphetamine and its stereoisomers in rhesus monkeys, J. Pharmacol. Exp. Ther. 334 (2) (2010) 642–650, https://doi.org/10.1124/jpet.110.166595.
[20] D.W. Curry, M.B. Young, A.N. Tran, G.E. Daoud, L.L. Howell, Separating the agony from ecstasy: R(–)-3,4-methylenedioxymethamphetamine has prosocial and therapeutic-like effects without signs of neurotoxicity in mice, Neuropharmacology 128 (2018) 196–206, https://doi.org/10.1016/j.neuropharm.2017.10.003.
[21] E. Acquas, A. Pisanu, S. Spiga, A. Plumitallo, G. Zernig, G.D. Chiara, Differential effects of intravenous R, S-(±)-3,4-methylenedioxymethamphetamine (MDMA, Ecstasy) and its S(+)- and R(–)-enantiomers on dopamine transmission and extracellular signal regulated kinase phosphorylation (pERK) in the rat nucleus accumbens shell and core, J. Neurochem. 102 (1) (2007) 121–132, https://doi.org/10.1111/j.1471-4159.2007.04451.x.
[22] N. Ameln, A. Ameln-Mayerhofer, Atypical development of behavioural sensitization to 3,4-methylenedioxymethamphetamine (MDMA, 'Ecstasy') in adolescent rats and its expression in adulthood: role of the MDMA chirality, Addict. Biol. 12 (1) (2010) 35–44, https://doi.org/10.1111/j.1369-1600.2009.00187.x.
[23] European Monitoring Centre for Drugs and Drug Addiction. *European Drug Report 2019: Trends and Developments*. Luxembourg: Publications Office of the European Union; 2019.
[24] European Monitoring Centre for Drugs and Drug Addiction. *European Drug Report 2020: Trends and Developments*. Luxembourg: Publications office of the European Union; 2020.
[25] P. Esseiva, S. Ioset, F. Anglada, L. Gasté, O. Ribaux, P. Margot, A. Gallusser, A. Biedermann, Y. Specht, E. Ottinger, Forensic drug intelligence: an important tool in law enforcement, Forensic Sci. Int. 167 (2–3) (2007) 247–254, https://doi.org/10.1016/j.forsciint.2006.06.032.
[26] Q. Milliet, C. Weyermann, P. Esseiva, The profiling of MDMA tablets: a study of the combination of physical characteristics and organic impurities as sources of information, Forensic Sci. Int. 187 (1–3) (2009) 58–65, https://doi.org/10.1016/j.forsciint.2009.02.017.
[27] R. Marquis, C. Weyermann, C. Delaporte, P. Esseiva, L. Aalberg, F. Besacier, J. S. Bozenko, R. Dahlenburg, C. Kopper, F. Zrcek, Drug intelligence based on MDMA tablets data: 2. Physical characteristics profiling, Forensic Sci. Int. 178 (1) (2008) 34–39, https://doi.org/10.1016/j.forsciint.2008.01.014.
[28] S.E.J. Bell, D.T. Burns, A.C. Dennis, L.J. Matchett, J.S. Speers, Composition profiling of seized ecstasy tablets by Raman spectroscopy, Analyst 125 (10) (2000) 1811–1815, https://doi.org/10.1039/b005662f.
[29] L.S.A. Pereira, F.L.C. Lisboa, J.C. Neto, F.N. Valladao, M.M. Sena, Screening method for rapid classification of psychoactive substances in illicit tablets using

mid infrared spectroscopy and PLS-DA, Forensic Sci. Int. 288 (2018) 227–235, https://doi.org/10.1016/j.forsciint.2018.05.001.
[30] K. Tsujikawa, K. Kuwayama, H. Miyaguchi, T. Kanamori, Y.T. Iwata, T. Yoshida, H. Inoue, Development of an on-site screening system for amphetamine-type stimulant tablets with a portable attenuated total reflection Fourier transform infrared spectrometer, Anal. Chim. Acta 608 (1) (2008) 95–103, https://doi.org/10.1016/j.aca.2007.12.002.
[31] J.Y.K. Cheng, M.F. Chan, T.W. Chan, M.Y. Hung, Impurity profiling of ecstasy tablets seized in Hong Kong by gas chromatography–mass spectrometry, Forensic Sci. Int. 162 (1–3) (2006) 87–94, https://doi.org/10.1016/j.forsciint.2006.02.055.
[32] C. Weyermann, R. Marquis, C. Delaporte, P. Esseiva, E. Lock, L. Aalberg, J. S. Bozenko, S. Dieckmann, L. Dujourdy, F. Zrcek, Drug intelligence based on MDMA tablets data: I. Organic impurities profiling, Forensic Sci. Int. 177 (1) (2008) 11–16, https://doi.org/10.1016/j.forsciint.2007.10.001.
[33] C. Koper, C. van den Boom, W. Wiarda, M. Schrader, P. de Joode, G. van der Peijl, A. Bolck, Elemental analysis of 3,4-methylenedioxymethamphetamine (MDMA): A tool to determine the synthesis method and trace links, Forensic Sci. Int. 171 (2-3) (2007) 171–179, https://doi.org/10.1016/j.forsciint.2006.11.003.
[34] M. Świst, J. Wilamowski, D. Zuba, J. Kochana, A. Parczewski, Determination of synthesis route of 1-(3,4-methylenedioxyphenyl)-2-propanone (MDP-2-P) based on impurity profiles of MDMA, Forensic Sci. Int. 149 (2–3) (2005) 181–192, https://doi.org/10.1016/j.forsciint.2004.06.016.
[35] C.M. Plummer, T.W. Breadon, J.R. Pearson, O.A.H. Jones, The synthesis and characterisation of MDMA derived from a catalytic oxidation of material isolated from black pepper reveals potential route specific impurities, Sci. Just. 56 (3) (2016) 223–230, https://doi.org/10.1016/j.scijus.2016.01.003.
[36] M. Świst, J. Wilamowski, A. Parczewski, Determination of synthesis method of ecstasy based on the basic impurities, Forensic Sci. Int. 152 (2–3) (2005) 175–184, https://doi.org/10.1016/j.forsciint.2004.08.003.
[37] A. Bolck, C. Weyermann, L. Dujourdy, P. Esseiva, J. Berg, Different likelihood ratio approaches to evaluate the strength of evidence of MDMA tablet comparisons, Forensic Sci. Int. 191 (1–3) (2009) 42–51, https://doi.org/10.1016/j.forsciint.2009.06.006.
[38] L. Patiny, M. Zasso, P. Esseiva, J. Wist, Seized ecstasy pills: infrared spectra and image datasets, Data 5 (4) (2020) 116, https://doi.org/10.3390/data5040116.
[39] P. Fagan, L. Kocourková, M. Tatarkovič, F. Králík, M. Kuchař, V. Setnička, P. Bouř, Cocaine hydrochloride structure in solution revealed by three chiroptical methods, ChemPhysChem. 18 (16) (2017) 2258–2265, https://doi.org/10.1002/cphc.201700452.
[40] D. Spálovská, F. Králík, M. Kohout, B. Jurásek, L. Habartová, M. Kuchař, V. Setnička, Structure determination of butylone as a new psychoactive substance using chiroptical and vibrational spectroscopies, Chirality 30 (5) (2018) 548–559, https://doi.org/10.1002/chir.v30.510.1002/chir.22825.
[41] D. Spálovská, T. Maříková, M. Kohout, F. Králík, M. Kuchař, V. Setnička, Methylone and pentylone: structural analysis of new psychoactive substances, Forensic Toxicol. 37 (1) (2019) 366–377, https://doi.org/10.1007/s11419-019-00489-8.
[42] N. Berova, P.L. Polavarapu, K. Nakanishi, R.W. Woody, Comprehensive Chiroptical Spectroscopy: Applications in Stereochemical Analysis of Synthetic Compounds, Natural Products, and Biomolecules, John Wiley & Sons, Inc., Hoboken, 2012.
[43] C.L. Covington, V.P. Nicu, P.L. Polavarapu, Determination of the absolute configurations using exciton chirality method for vibrational circular dichroism: right answer for the wrong reason? J. Phys. Chem. A 119 (42) (2015) 10589–10601, https://doi.org/10.1021/acs.jpca.5b07940.
[44] F. Králík, P. Fagan, M. Kuchař, V. Setnička, Structure of heroin in a solution revealed by chiroptical spectroscopy, Chirality. 32 (6) (2020) 854–865, https://doi.org/10.1002/chir.v32.610.1002/chir.23196.
[45] D.M. McCann, P.J. Stephens, Determination of absolute configuration using density functional theory calculations of optical rotation and electronic circular dichroism: chiral alkenes, J. Org. Chem. 71 (16) (2006) 6074–6098, https://doi.org/10.1021/jo060755.
[46] D. Spálovská, M. Paškan, B. Jurásek, M. Kuchař, M. Kohout, V. Setnička, Structural spectroscopic study of enantiomerically pure synthetic cathinones and their major metabolites, New J. Chem. 45 (2) (2021) 850–860, https://doi.org/10.1039/D0NJ05065B.
[47] B. Jurásek, F. Králík, S. Rimpelová, J. Čejka, V. Setnička, T. Ruml, M. Kuchař, M. Kohout, Synthesis, absolute configuration and in vitro cytotoxicity of deschloroketamine enantiomers: Rediscovered and abused dissociative anaesthetic, New J. Chem. 42 (24) (2018) 19360–19368, https://doi.org/10.1039/C8NJ03107J.
[48] M. Urbanová, V. Setnička, K. Volka, Measurements of concentration dependence and enantiomeric purity of terpene solutions as a test of a new commercial VCD spectrometer, Chirality 12 (4) (2000) 199–203, https://doi.org/10.1002/(SICI)1520-636X(2000)12:4<199::AID-CHIR6>3.0.CO;2-L.
[49] P. Fagan, D. Spálovská, R. Jurok, M. Kuchař, V. Schrenková, V. Setnička, Structural analysis of MDMA in solution by methods of chiroptical spectroscopy supported by DFT calculations, Vib. Spectrosc. 114 (2021) 103255, https://doi.org/10.1016/j.vibspec.2021.103255.
[50] P.L. Polavarapu, E. Santoro, Vibrational optical activity for structural characterization of natural products, Nat. Prod. Rep. 37 (12) (2020) 1661–1699, https://doi.org/10.1039/D0NP00025F.
[51] L.A. Nafie, Vibrational circular dichroism: a new tool for the solution-state determination of the structure and absolute configuration of chiral natural product molecules, Nat. Prod. Commun. (2008), https://doi.org/10.1177/1934578X0800300322.
[52] L. Kong, P. Wang, Determination of the absolute configuration of natural products, Chin. J. Nat. Med. 11 (3) (2013) 193–198, https://doi.org/10.1016/S1875-5364(13)60016-3.
[53] R.E. Río, P. Joseph-Nathan, Vibrational circular dichroism absolute configuration of natural products from 2015 to 2019, Nat. Prod. Commun. 2021 (2015), https://doi.org/10.1177/1934578X21996166.
[54] P.J. Stephens, F.J. Devlin, J.J. Pan, The determination of the absolute configurations of chiral molecules using vibrational circular dichroism (VCD) spectroscopy, Chirality 20 (5) (2008) 643–663, https://doi.org/10.1002/chir.20477.